Original Article

Changes in right ventricular function on three-dimensional speckle tracking echocardiography after transcatheter pulmonary valve replacement

Mengmeng Ji[1,2,3#], Wenqian Wu[1,2,3#], Mingxing Xie[1,2,3#], Li Zhang[1,2,3#], Yixia Lin[1,2,3], Lang Gao[1,2,3], Qing He[1,2,3], Nianguo Dong[4], Yuman Li[1,2,3]

[1]Department of Ultrasound Medicine, Union Hospital, Tongji Medical College, Huazhong University of Science and Technology, Wuhan, China; [2]Clinical Research Center for Medical Imaging in Hubei Province, Wuhan, China; [3]Hubei Province Key Laboratory of Molecular Imaging, Wuhan, China; [4]Department of Cardiovascular Surgery, Union Hospital, Tongji Medical College, Huazhong University of Science and Technology, Wuhan, China

Contributions: (I) Conception and design: M Ji, W Wu, M Xie, L Zhang; (II) Administrative support: M Xie, L Zhang, N Dong, Y Li; (III) Provision of study materials or patients: M Ji, Y Lin, L Gao, Q He; (IV) Collection and assembly of data: M Ji, Y Lin, Q He; (V) Data analysis and interpretation: W Wu, L Gao, Q He; (VI) Manuscript writing: All authors; (VII) Final approval of manuscript: All authors.

[#]These authors contributed equally to this work.

Correspondence to: Nianguo Dong, MD, PhD. Department of Cardiovascular Surgery, Union Hospital, Tongji Medical College, Huazhong University of Science and Technology, 1277 Jiefang Avenue, Wuhan 430022, China. Email: dongnianguo@hotmail.com; Yuman Li, MD, PhD. Department of Ultrasound Medicine, Union Hospital, Tongji Medical College, Huazhong University of Science and Technology, 1277 Jiefang Avenue, Wuhan 430022, China; Clinical Research Center for Medical Imaging in Hubei Province, Wuhan, China; Hubei Province Key Laboratory of Molecular Imaging, Wuhan, China. Email: liym@hust.edu.cn.

Background: Pulmonary regurgitation (PR) is common after tetralogy of Fallot (TOF) repair and closely associated with adverse outcomes. Transcatheter pulmonary valve replacement (TPVR) is a novel treatment for severe PR or mixed pulmonary stenosis (PS) and regurgitation. The aim of this study was to evaluate the changes in right ventricular (RV) function in patients after TPVR on two-dimensional (2D) and three-dimensional (3D) speckle tracking echocardiography and to identify the predictors of RV function and New York Heart Association (NYHA) functional class at 6 months after TPVR.

Methods: Twenty-one patients who underwent TPVR were prospectively enrolled. 2D and 3D RV free wall longitudinal strain (2D-RVFWLS and 3D-RVFWLS) were obtained by 2D and 3D speckle tracking echocardiography, respectively, before TPVR and at 1 week and 6 months after TPVR.

Results: The 2D-RVFWLS and 3D-RVFWLS at 1 week after TPVR were lower than those before TPVR and improved to the baseline levels at 6 months after TPVR ($P<0.05$). Preoperative 2D-RVFWLS and 3D-RVFWLS were independent predictors of RV function ($\beta=0.415$ and $\beta=0.618$; $P<0.05$) and NYHA functional class ($\beta=0.636$ and $\beta=0.674$; $P<0.05$) at 6 months after TPVR. In predicting RV function at 6 months after TPVR, the model with 3D-RVFWLS ($R^2=0.606$; $P=0.008$) was not inferior to that with 2D-RVFWLS ($R^2=0.424$; $P=0.034$). Moreover, in predicting NYHA functional class at 6 months after TPVR, the model with 3D-RVFWLS ($R^2=0.771$; $P<0.001$) was similar to that with 2D-RVFWLS ($R^2=0.737$; $P<0.001$).

Conclusions: 2D-RVFWLS and 3D-RVFWLS decreased 1 week after TPVR and returned to the baseline levels at 6-month follow-up. Preoperative 2D-RVFWLS and 3D-RVFWLS are independent predictors of RV function and NYHA functional class at 6 months after TPVR.

Keywords: Transcatheter pulmonary valve replacement (TPVR); speckle tracking echocardiography; right

ventricular function (RV function)

Submitted Apr 10, 2025. Accepted for publication Sep 01, 2025. Published online Oct 24, 2025.
doi: 10.21037/qims-2025-863
View this article at: https://dx.doi.org/10.21037/qims-2025-863

Introduction

Tetralogy of Fallot (TOF) is the most common cause of cyanotic congenital heart disease (1) and is usually treated by surgical transannular patch repair. Pulmonary regurgitation (PR) is common after TOF repair and is closely associated with late right ventricular (RV) outflow tract dilatation, RV dysfunction, tricuspid valve regurgitation, arrhythmias, and sudden death (2-6). Therefore, timely intervention of PR is critical to modifying the natural processes of the disease and improving the prognosis. For patients with high risk or contraindications to surgery, transcatheter pulmonary valve replacement (TPVR) may serve as a desirable alternative to surgical pulmonary valve replacement (PVR), which is associated with high risk, major injury, and a high frequency of complications (7-10). TPVR can relieve symptoms, reverse RV reconstruction, improve cardiac function and delay, and reduce the number of open-heart surgeries, thus prolonging life expectancy (7). The European Society of Cardiology guidelines indicate that TPVR is the first choice of treatment for patients with repaired TOF and PR (11).

RV function after TPVR is closely related to prognosis, and therefore accurate assessment of RV function before TPVR and during postoperative follow-up can aid clinicians in determining the timing of operative intervention and adjusting the treatment plan in a timely manner. Cardiac magnetic resonance, the gold standard for evaluating RV function, has disadvantages including the influence of stent-valve artifacts, high cost, long scanning time, and contraindication of metal implants (12). Echocardiography can circumvent these limitations while having the advantages of being low cost, simple to operate, time-saving, and amenable to bedside use; it is thus the preferred examination method for patients after TPVR (13). However, the complex geometry of the RV complicates the evaluation of RV function by conventional echocardiography. Two-dimensional speckle tracking echocardiography (2D-STE) is angle-independent, easy to use, and highly repeatable (14,15). A large body of evidence indicates that 2D-STE parameters are more sensitive in detecting subclinical RV dysfunction than are conventional RV echocardiographic parameters. However, 2D-STE is limited by the out-of-plane motion of the speckles as cardiac motion is three-dimensional (3D) in nature. Previous studies using 2D-STE to evaluate the changes in RV function after TPVR have produced inconsistent results, with two-dimensional (2D) RV strain improving, worsening, or returning to the preoperative baseline levels (16). Three-dimensional speckle tracking echocardiography (3D-STE) based on real-time full-volume scanning can overcome the limitations of 2D-STE and evaluate myocardial function more accurately and objectively (14,15,17-19). However, thus far, no study has used 3D-STE to monitor the changes in RV function after TPVR.

Therefore, we conducted a study to (I) evaluate RV function at 6 months after TPVR using 2D-STE and 3D-STE; (II) investigate the predictors of RV function and New York Heart Association (NYHA) functional class at 6 months after TPVR; and (III) directly compare the value of 2D-STE and 3D-STE parameters in predicting RV function and NYHA functional class after TPVR. We present this article in accordance with the STROBE reporting checklist (available at https://qims.amegroups.com/article/view/10.21037/qims-2025-863/rc).

Methods

Study population

A total of 40 patients with repaired TOF with moderate or severe PR were prospectively enrolled in our study between September 2021 and December 2023 at Union Hospital in Wuhan, China. The inclusion criteria (20,21) were as follows: (I) age ≥5 years; (II) weight ≥35 kg; (III) previous TOF repair; (IV) original conduit diameter ≥16 mm; and (V) NYHA functional class ≥II with moderate or severe PR or NYHA functional class I with severe PR. Moderate PR was defined as a regurgitant color Doppler jet width of 20% to 40% of the valve annulus or diastolic flow reversal extending into the distal main pulmonary artery. Severe PR was defined as a regurgitant color Doppler jet width >40% of the valve annulus or diastolic flow reversal extending into the branch pulmonary arteries. The exclusion criteria were as follows: (I) age <5 years; (II) weight <35 kg; (III) poor image quality prohibiting speckle tracking analysis; and (IV) loss to follow-up. Among the 30 patients with TPVR, 3 patients with poor image quality and 6 patients that were lost to follow-up were excluded. Finally, 21 patients with TPVR were included in this study, including 17 (81.0%) with PR alone and 4 (19.0%) with PR combined with pulmonary stenosis (PS). Additionally, 24 healthy volunteers were enrolled as a control group under the following exclusion criteria: complicated with cardiovascular disease or other systemic diseases, nonsinus rhythm, and poor image quality during the examination. This study was approved by the Ethics Committee of Wuhan Union Hospital, Tongji Medical College, Huazhong University of Science and Technology (No. UHCT-IEC-SOP-016-03-03) and conformed to the principles outlined in the Declaration of Helsinki and its subsequent amendments. In addition, all participants signed a written informed consent prior to enrollment.

Echocardiography

All comprehensive echocardiographic examinations were performed with EPIQ7C ultrasound machine (Philips Medical Systems, Best, the Netherlands). Echocardiograms for the TPVR and control groups were acquired by experienced sonographers according to the protocol for the evaluation of cardiac function. The echocardiographic examinations were performed before TPVR and at 1 week and 6 months after TPVR. All participants were placed in the left lateral decubitus position, and the electrocardiography was recorded simultaneously. An RV-focused apical four-chamber view with a frame rate of >50 frames/s was used for the 2D-STE analysis. The 3D echocardiographic data were obtained with an RV-focused apical four-chamber view in full-volume mode with four consecutive cardiac cycles at a volume rate of >20 volumes/s.

Conventional echocardiographic measurements were based on the guidelines of the American Society of Echocardiography and the European Association for Cardiovascular Imaging (22,23). RV base diameter, mid-diameter. and longitudinal diameter were acquired from the RV-focused apical four-chamber view. Tricuspid annular plane systolic excursion (TAPSE) was obtained via M-mode echocardiography with a cursor positioned at the junction of the lateral tricuspid leaflet and the RV free wall. Pulmonary artery systolic pressure was calculated according to the maximum velocity of the tricuspid regurgitant jet obtained from continuous wave Doppler and integrated into the modified Bernoulli equation and the right atrial pressure. Right atrial pressure was evaluated based on the diameter of the inferior vena cava and its collapsibility (24). RV end-diastolic and end-systolic areas were calculated from the RV-focused apical four-chamber view for measurement of the RV fractional area change (RVFAC), which was calculated as follows: RVFAC = [(RV end-diastolic area – RV end-systolic area)/RV end-diastolic area] × 100%. Tricuspid annular systolic excursion velocity (S'), early diastolic velocity, and late diastolic velocity were obtained via tissue Doppler imaging in the RV-focused apical four-chamber view. Left ventricular ejection fraction (LVEF) was estimated via the biplane Simpson method. PR was graded from 0 to 4 based on the basis of the jet width: annulus ratio and flow reversal in the branch pulmonary arteries as follows—0= no regurgitation, 1= jet width: annulus ratio <0.25, 2= jet width: annulus ratio between 0.25 and 0.5, 3= jet width: annulus ratio between 0.5 and 0.7, and 4= jet width: annulus >0.7 with flow reversal in the branch pulmonary arteries (25,26).

Speckle tracking echocardiography

Two-dimensional and three-dimensional transthoracic echocardiographic images were digitally stored for offline analysis through the Tomtec 4.0 workstation (TOMTEC Imaging Systems GmbH, Unterschleissheim, Germany) by a single experienced investigator blinded to the patients' clinical data.

Two-dimensional speckle tracking echocardiography

The 2D-STE analysis was performed in the RV-focused apical four-chamber view. Locating points were respectively placed on the endocardium of the RV free wall side and the interventricular septum side of the tricuspid annulus and the RV apex (*Figure 1A,1B*). Subsequently, software was used to automatically segment the RV into six segments (basal, middle, and apical segments of both the RV free wall and the interventricular septum) and track the myocardial speckle motion throughout the cardiac cycle. The endocardial boundary was manually modified by the operator if the tracking was insufficient. Finally, RV longitudinal strain curves of the free wall and septum were automatically generated by the software (*Figure 1C*). Two-dimensional RV free wall longitudinal strain (2D-RVFWLS)

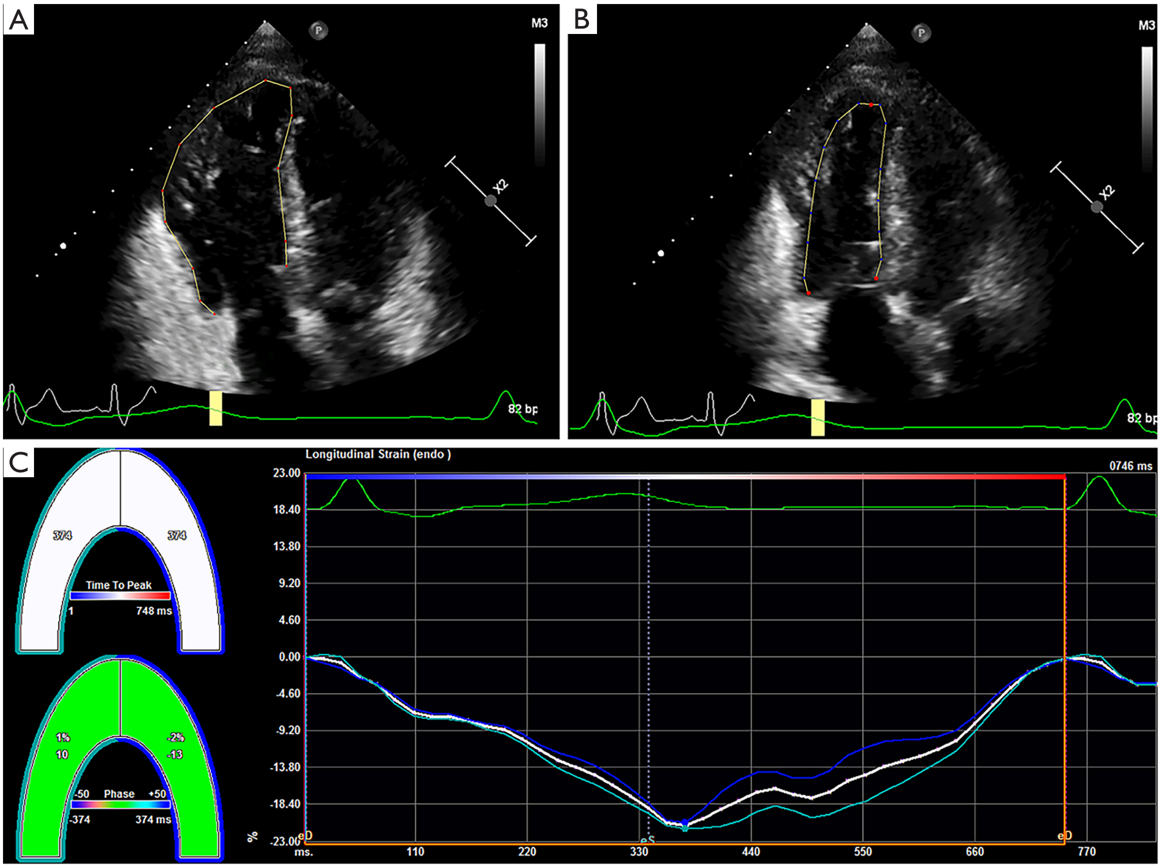

Figure 1 Two-dimensional speckle tracking echocardiography analysis of the right ventricle. Tomtec software identifies and tracks the right ventricular endocardium in end diastole (A) and end systole (B). Two-dimensional longitudinal strain of the right ventricular free wall and septum is automatically generated (C).

was calculated as the average value of the longitudinal strain of the basal, middle, and apical segments of the RV free wall. After exclusion of 6 patients who were lost to follow-up, 24 out of 30 patients underwent 2D-STE analysis. Manual adjustments of the endocardial boundaries were made in the 10 patients with poor image quality. After the adjustment, 1 patient was still excluded due to the image quality being too poor for 2D-STE analysis. Therefore, the feasibility rate of 2D-STE analysis in patients with repaired TOF in terms of suboptimal windows and subsequent need for manual adjustments was 90%.

Three-dimensional speckle tracking echocardiography

Three-dimensional full-volume data were analyzed via four-dimensional RV function analysis software (Tomtec). The most appropriate cardiac cycle with the clearest endocardial delineation was selected for analysis. In the apical two-chamber and four-chamber views at the end-diastolic frame, the largest apical long-axis dimensions were determined by selecting the point of the left ventricular apex and the center of the mitral annular line. In the RV-focused apical four-chamber and coronal views, the point of the RV apex and the center of the tricuspid annular line were determined. The operator placed landmarks corresponding to the aortic annulus diameter in the apical three-chamber view. In the RV short-axis view, the anterior and posterior junctions of the RV free wall with the interventricular septum and the distance from the septum to the RV free wall were identified (*Figure 2A*). The software automatically delineated the endocardial border and tracked it throughout the cardiac cycle, and the investigator could manually adjust the end-diastolic (*Figure 2B*) and end-systolic (*Figure 2C*) endocardial boundaries if tracking was unsatisfactory. The RV volume-time curve (*Figure 2D*), RV end-diastolic volume (RVEDV), RV end-systolic volume (RVESV), and

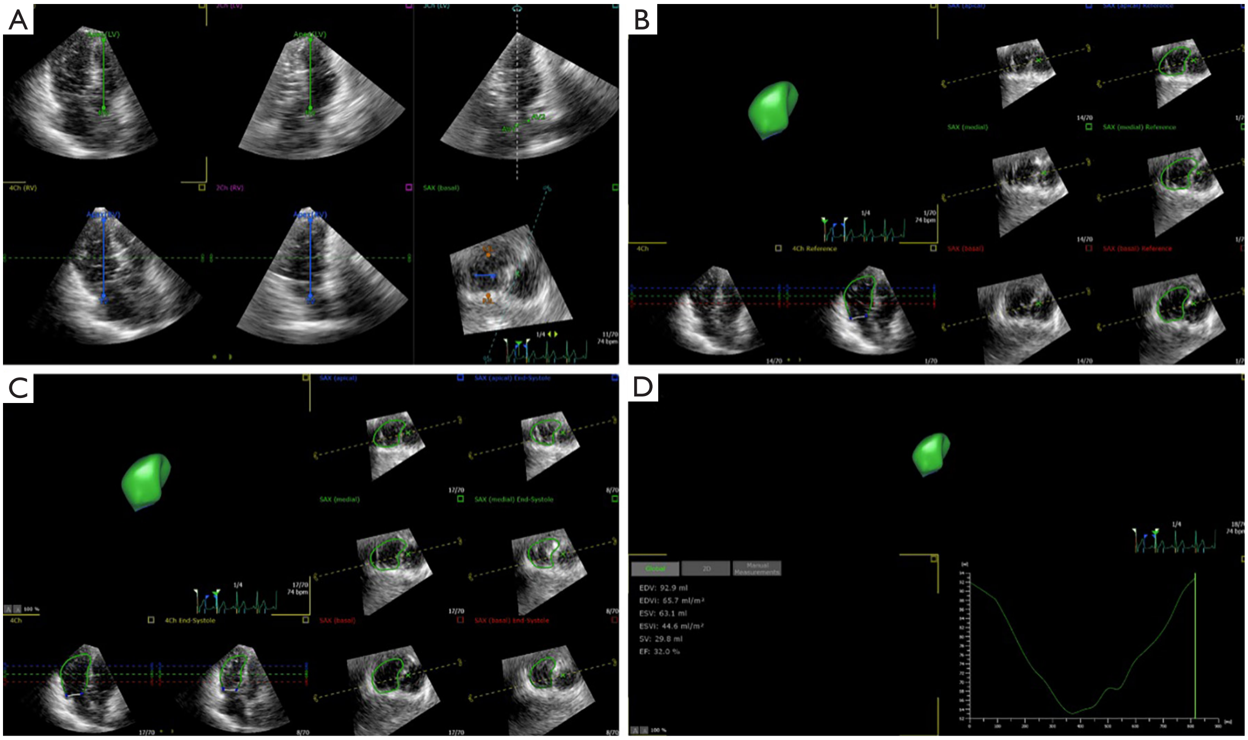

Figure 2 Three-dimensional speckle tracking echocardiography analysis of right ventricle. (A) Setting of the reference points. (B,C) Right ventricular endocardial border tracking. (D) The three-dimensional longitudinal strain of the right ventricular free wall and septum is automatically generated.

RV ejection fraction (RVEF) were automatically generated. Additionally, the software automatically generated the RV strain-time curve and 3D RV free wall longitudinal strain (3D-RVFWLS). After exclusion of 6 patients who were lost to follow-up, 24 out of 30 patients underwent 3D-STE analysis. Manual adjustments of the end-diastolic and end-systolic endocardial boundaries were made in the 15 patients with poor image quality. After the adjustment, 3 patients (including the 1 patient above who could not undergo 2D-STE analysis) were still excluded because the image quality was too poor for 3D-STE analysis. Therefore, the feasibility rate of 3D-STE analysis in patients with repaired TOF in terms of suboptimal windows and subsequent need for manual adjustments was 80%, which was inferior to that of 2D-STE analysis.

Intra- and interobserver reproducibility analysis

To examine the intra-and interobserver variability of 2D-RVFWLS and 3D-RVFWLS, we randomly selected 20 patients and estimated the reproducibility of 2D-RVFWLS and 3D-RVFWLS by means of Bland-Altman analysis and the intraclass correlation coefficient. For intraobserver variability, the data were reanalyzed independently by the same investigator after 2 weeks. For interobserver variability, the data were analyzed by another experienced investigator who was blinded to the values obtained by the first investigator.

Statistical analysis

Continuous variables are expressed as the mean ± standard deviation or as the median and interquartile range (IQR). Categorical variables are expressed as frequency (percentage). The Shapiro-Wilk normality test was used to test the normal distribution of the data. Comparisons of parameters between the TPVR group and the control group were performed with the independent samples *t*-test (for normally distributed data), the Mann-Whitney test (for nonnormally distributed data), or the Chi-squared test or Fisher exact test (for categorical variables). Preoperative and postoperative cardiac catheterization parameters

Table 1 Clinical data in the TPVR and control groups

Variable	TPVR group (n=21)	Control group (n=24)	P value
Age, years	27 [19, 49]	26 [24, 46]	0.553
Age of first TOF repair, years	7 [3, 14]	–	–
Male	14 (66.7)	15 (62.5)	0.967
Height, cm	163.9±8.7	167.5±7.8	0.186
Weight, kg	62.8±15.2	65.6±11.2	0.288
BMI, kg/m^2	22.6±4.8	23.3±2.8	0.552
Systolic blood pressure, mmHg	115±17	122±9	0.086
Diastolic blood pressure, mmHg	76±13	75±7	0.931
TPVR indication		–	–
PR	17 (81.0)	–	–
PR + PS	4 (19.0)	–	–
PR grading		–	–
3+ (moderate to severe)	2 (9.5)	–	–
4+ (severe)	19 (90.5)	–	–
NYHA class ≥II before TPVR	18 (85.7)	–	–
NYHA class ≥II at 6 months after TPVR	15 (71.4)	–	–
Heart rate before TPVR, bpm	81±19	–	–
PR interval before TPVR, ms	156.7±22.1	–	–
QRS duration before TPVR, ms	162.7±35.1	–	–

Data are expressed as the mean ± standard deviation, number (%), or as the median [range]. BMI, body mass index; NYHA, New York Heart Association; PR, pulmonary regurgitation; PS, pulmonary stenosis; TOF, tetralogy of Fallot; TPVR, transcatheter pulmonary valve replacement.

were compared via the paired-samples *t*-test or Wilcoxon test. Echocardiographic parameters before and 1 week and 6 months after TPVR were compared via repeated-measures analysis of variance or the Kruskal-Wallis test. Correlations between the parameters were assessed with Pearson or Spearman correlation coefficient. Univariate and multiple linear regression analyses were used to determine the predictors of RV function and NYHA functional class at 6 months after TPVR. The variables with P<0.05 in the univariate linear regression analysis with clinical significance were included in the multiple linear regression model. Bland-Altman analysis and the intraclass correlation coefficient were used to assess the reproducibility of 2D-RVFWLS and 3D-RVFWLS. Statistical analyses were performed with SPSS 26.0 (IBM Corp., Armonk, NY, USA) and GraphPad Prism 8.0.1 (Dotmatics, Boston, MA, USA). A two-tailed P<0.05 was considered statistically significant.

Results

Clinical characteristics

The clinical characteristics of the TPVR group and the control group are shown in *Table 1*. A total of 21 patients with a median age of 27 (IQR, 19–49) years underwent TPVR, and 14 (66.7%) patients were male. Among these patients, there were 17 (81.0%) with PR alone and 4 (19.0%) with PR combined with PS. There were 2 (9.5%) patients with moderate-to-severe PR and 19 (90.5%) with severe PR. Furthermore, 18 (85.7%) patients had NYHA functional class ≥II before TPVR, and 15 (71.4%) had NYHA functional class ≥II at 6 months after TPVR. Additionally, 24 healthy volunteers were enrolled as the

Table 2 The preoperative and immediately postoperative right cardiac catheterization parameters

Variable	Pre-TPVR	Post-TPVR	P value
PASP, mmHg	30.6±7.4	27.2±9.2	0.044
RV systolic pressure, mmHg	34.5±14.4	31.5±9.5	0.038
RV-PA pressure gradient, mmHg	7.7±16.1	4.2±6.6	0.033

Data are expressed as the mean ± standard deviation. PA, pulmonary artery; PASP, pulmonary artery systolic pressure; RV, right ventricular; TPVR, transcatheter pulmonary valve replacement.

control group, including 15 (62.5%) males and 9 (37.5%) females, with a median age of 26 (IQR, 24–46) years. Age, sex, height, weight, body mass index, and blood pressure did not differ significantly between the TPVR and control groups (P>0.05).

Right heart catheterization parameters

The comparison of preoperative and immediately postoperative right heart catheterization parameters in the TPVR group is summarized in *Table 2*. Pulmonary artery systolic pressure decreased from 30.6±7.4 mmHg preoperatively to 27.2±9.2 mmHg postoperatively, RV systolic pressure decreased from 34.5±14.4 mmHg preoperatively to 31.5±9.5 mmHg postoperatively, and the RV-pulmonary artery pressure gradient decreased from 7.7±16.1 mmHg preoperatively to 4.2±6.6 mmHg postoperatively.

Echocardiographic characteristics

The echocardiographic characteristics before TPVR and at 1 week and 6 months after TPVR are shown in *Table 3* and *Figure 3*. RV base diameter and RVEDV at 1 week and 6 months after TPVR were significantly decreased as compared with preoperative values but and were still higher than those in the control group. The 2D-RVFWLS and 3D-RVFWLS at 1 week after TPVR were significantly lower than those before TPVR and gradually improved to the baseline levels at 6 months after TPVR; however, they were still lower than those in the control group (P<0.05). RVFAC, TAPSE, S’, pulmonary artery systolic pressure, RVEF, left atrial diameter, left ventricular end-diastolic diameter, and LVEF before TPVR did not differ significantly at 1 week or 6 months after TPVR (P>0.05).

Correlation between 3D-RVFWLS and 2D-RVFWLS

The correlation data between 3D-RVFWLS and 2D-RVFWLS in patients with TPVR are shown in *Figure 4*. Preoperative 3D-RVFWLS was strongly associated with 2D-RVFWLS before TPVR (r=0.774; P<0.001), 3D-RVFWLS at 1 week after TPVR was strongly associated with 2D-RVFWLS at 1 week after TPVR (r=0.857; P<0.001), and 3D-RVFWLS at 6 months after TPVR was moderately correlated with 2D-RVFWLS at 6 months after TPVR (r=0.662; P=0.001).

Relationship between 3D-RVFWLS 6 months after TPVR and baseline echocardiographic indices

The data for the correlation between 3D-RVFWLS at 6 months after TPVR and baseline echocardiographic indices are shown in *Table 4* and *Figure 5*. The 3D-RVFWLS at 6 months after TPVR was strongly correlated with the 3D-RVFWLS before TPVR (r=0.756; P<0.05) and moderately correlated with the RV end-systolic area (r=0.525; P=0.015), RVEDV (r=0.598; P=0.004), RVESV (r=0.636; P=0.002), and 2D-RVFWLS (r=0.543; P=0.011) before TPVR. Meanwhile, the 3D-RVFWLS at 6 months after TPVR was not associated with LVEF, RV end-diastolic area, RVFAC, TAPSE, S’, or RVEF (P>0.05).

Predictors of RV function at 6 months after TPVR

Univariate regression analysis showed that QRS duration (β=0.581; P<0.001), RV end-systolic area (β=0.545; P=0.011), RVEDV (β=0.598; P=0.004), RVESV (β=0.616; P=0.003), 2D-RVFWLS (β=0.623; P=0.001), and 3D-RVFWLS (β=0.756; P<0.001) before TPVR were predictors of 3D-RVFWLS at 6 months after TPVR. Multivariate linear regression analysis demonstrated that preoperative 2D-RVFWLS (β=0.415; P=0.034) and 3D-RVFWLS (β=0.618; P=0.008) were independent predictors of 3D-RVFWLS at 6 months after TPVR (*Table 5*). The model with 3D-RVFWLS (R^2=0.606; P=0.008) was not inferior to 2D-RVFWLS at predicting RV function at 6 months after TPVR (R^2=0.424; P=0.034).

Table 3 Echocardiography parameters before and after TPVR

Variable	Pre-TPVR (n=21)	1 week (n=21)	6 months (n=21)	Control group (n=24)	P value
Left heart parameters					
LA diameter, mm	36.0 (29.0, 41.0)	33.0 (30.0, 43.5)	35.5 (32.3, 41.5)§	31.0 (29.0, 33.8)	0.027
LVEDD, mm	44.8±6.2	46.8±7.0§	47.2±5.8§	43.0±3.5	0.065
LVESD, mm	29.0 (27.0, 33.0)§	29.5 (26.5, 34.0)§	29.5 (26.3, 36.0)§	24.5 (21.0, 27.0)	<0.001
LVEF, %	64.0 (57.0, 68.0)§	65.0 (59.3, 66.8)§	66.0 (63.0, 69.0)§	71.0 (67.0, 73.0)	<0.001
MV E, m/s	0.9 (0.8, 1.1)	0.9 (0.7, 0.9)	1.0 (0.8, 1.1)	0.9 (0.8, 1.0)	0.557
MV A, m/s	0.6 (0.5, 0.8)	0.7 (0.5, 0.8)	0.6 (0.6, 0.8)	0.7 (0.5, 0.8)	0.848
MV E/A	1.5±0.5	1.4±0.4	1.5±0.4	1.5±0.4	0.565
MV E/e'	6.9 (6.0, 12.0)	7.0 (6.0, 9.9)	8.4 (6.5, 10.5)	9.1 (7.7, 10.6)	0.126
Right heart parameters					
RA diameter, mm	47.0 (41.5, 56.0)§	45.0 (39.3, 52.0)§	43.5 (37.3, 52.0)§	32.5 (32.0, 34.8)	<0.001
RVD1, mm	53.1±11.1§	48.1±10.3†,§	44.6±9.3†,§	32.0±2.2	<0.001
RVD2, mm	49.7±10.4§	47.2±10.8§	44.6±7.7§	29.8±4.3	<0.001
RVD3, mm	89.0 (84.0, 98.0)§	90.0 (82.3, 96.8)§	85.5 (77.0, 90.0)§	73.7 (67.3, 76.5)	<0.001
TV E, m/s	0.8 (0.6, 1.0)	0.8 (0.6, 1.0)	0.9 (0.7, 1.0)§	0.6 (0.5, 0.7)	0.032
TV A, m/s	0.5 (0.4, 0.6)	0.4 (0.4, 0.6)	0.6 (0.4, 0.6)	0.4 (0.4, 0.5)	0.087
TV E/A	1.4 (1.3, 1.8)	1.5 (1.3, 2.1)	1.5 (1.3, 1.8)	1.4 (1.3, 1.8)	0.625
PV velocity, m/s	1.7 (1.2, 2.4)§	1.6 (1.3, 2.0)§	1.9 (1.7, 2.2)§	1.0 (0.9, 1.1)	<0.001
PV pressure difference, mmHg	11.0 (5.8, 22.8)§	10.0 (7.0, 15.3)§	14.5 (11.0, 18.8)§	4.0 (3.0, 5.0)	<0.001
PASP, mmHg	32.0 (25.0, 41.0)§	30.0 (27.0, 37.0)§	30.0 (26.3, 33.8)§	23.0 (21.0, 25.0)	<0.001
RVOT diameter, mm	34.0 (28.5, 40.0)§	34.5 (29.3, 42.3)§	34.0 (30.0, 37.8)§	20.0 (18.3, 22.0)	<0.001
RVEDA, cm^2	35.0 (29.0, 39.5)§	30.1 (23.0, 37.1)§	24.9 (20.5, 35.4)§	14.1 (12.8, 15.1)	<0.001
RVESA, cm^2	20.2 (17.9, 24.9)§	17.8 (14.7, 22.4)§	14.2 (11.8, 21.8)§	7.2 (6.2, 8.2)	<0.001
RVFAC, %	38.9±7.1§	37.3±7.2§	40.1±5.7§	48.6±5.0	<0.001
TAPSE, mm	16.2±3.0§	13.8±2.8§	15.4±2.6§	22.3±2.7	<0.001
S', cm/s	12.6±2.4§	9.4±1.7§	11.3±2.1§	14.9±2.8	<0.001
2D-RVFWLS, %	–19.3±4.8§	–16.3±4.8†,§	–21.5±4.7‡,§	–29.2±2.9	<0.001
RVEDV, mL	193.7±43.8§	143.9±46.7†,§	121.4±41.3†,§	76.5±16.7	<0.001
RVESV, mL	99.5 (72.9, 133.8)§	81.7 (55.2, 115.7)	61.3 (46.4, 90.2)†,§	30.9 (27.8, 38.6)	<0.001
RVEF, %	45.5±8.5§	39.0±7.8§	45.4±9.6§	56.2±6.7	<0.001
3D-RVFWLS, %	–21.1±3.8§	–18.7±4.6†,§	–25.4±4.6‡,§	–32.0±3.5	<0.001

Data are expressed as the mean ± standard deviation or as the median (range). †, compared with pre-TPVR values; ‡, compared with 1 week after TPVR; §, compared with control. 2D-RVFWLS, two-dimensional right ventricular free wall longitudinal strain; 3D-RVFWLS, three-dimensional right ventricular free wall longitudinal strain; LA, left atrium; LVEDD, left ventricular end-diastolic diameter; LVEF, left ventricular ejection fraction; LVESD, left ventricular end-systolic diameter; MV, mitral valve; PASP, pulmonary artery systolic pressure; PV, pulmonary valve; RA, right atrium; RVD1, right ventricular base diameter; RVD2, right ventricular mid-diameter; RVD3, right ventricular length diameter; RVEDA, right ventricular end-diastolic area; RVEDV, right ventricular end-diastolic volume; RVESA, right ventricular end-systolic area; RVESV, right ventricular end-systolic volume; RVFAC, right ventricular fractional area change; RVOT, right ventricular outflow tract; S’, tricuspid annular systolic excursion velocity; TAPSE, tricuspid annular plane systolic excursion; TPVR, transcatheter pulmonary valve replacement; TV, tricuspid valve.

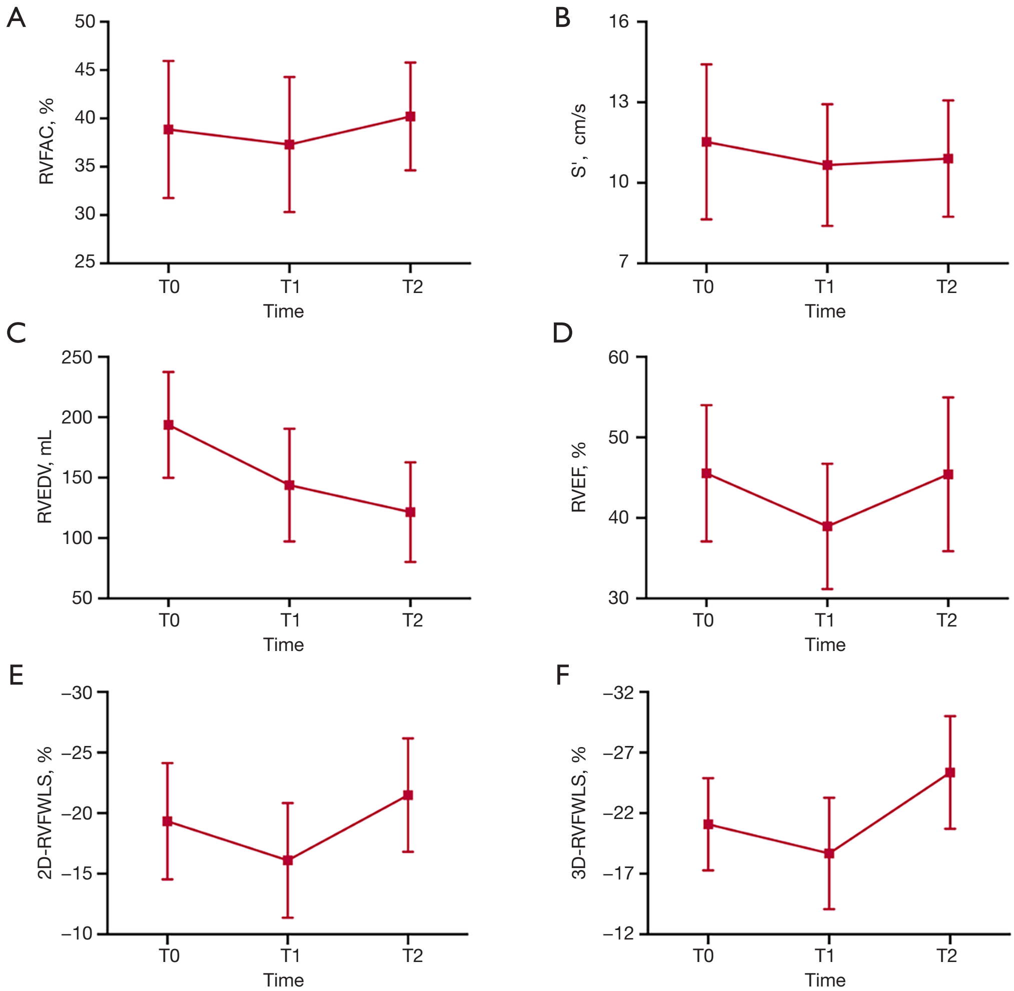

Figure 3 Line graph of changes in the right ventricular echocardiographic parameters before and after TPVR. (A) RVFAC. (B) S'. (C) RVEDV. (D) RVEF. (E) 2D-RVFWLS. (F) 3D-RVFWLS. 2D-RVFWLS, two-dimensional right ventricular free wall longitudinal strain; 3D-RVFWLS, three-dimensional right ventricular free wall longitudinal strain; RVEDV, right ventricular end-diastolic volume; RVEF, right ventricular ejection fraction; RVFAC, right ventricular fractional area change; S', tricuspid annular systolic excursion velocity; T0, before TPVR; T1, 1 week after TPVR; T2, 6 months after TPVR; TPVR, transcatheter pulmonary valve replacement.

Predictors of NYHA class at 6 months after TPVR

Univariate regression analysis demonstrated that preoperative RVEDV (β=0.605; P=0.004), RVESV (β=0.713; P<0.001), RVEF (β=−0.557; P=0.009), 2D-RVFWLS (β=0.778; P<0.001), and 3D-RVFWLS (β=0.828; P<0.001) were predictors of NYHA functional class at 6 months after TPVR. Multivariate linear regression analysis showed that preoperative 2D-RVFWLS (β=0.636; P<0.001) and 3D-RVFWLS (β=0.674; P<0.001) were independent predictors of NYHA functional class at 6 months after TPVR (*Table 6*). In predicting NYHA functional class at 6 months after TPVR, the model with 3D-RVFWLS (R^2=0.771; P<0.001) was similar to that with 2D-RVFWLS (R^2=0.737; P<0.001).

Reproducibility

The inter- and the intraobserver reproducibility of 2D-RVFWLS and 3D-RVFWLS were excellent, as reflected by the high intraclass correlation coefficient. In addition, Bland-Altman analysis demonstrated high intra- and interobserver agreement, with low bias and narrow limits of agreement (*Table* 7 and *Figure 6*).

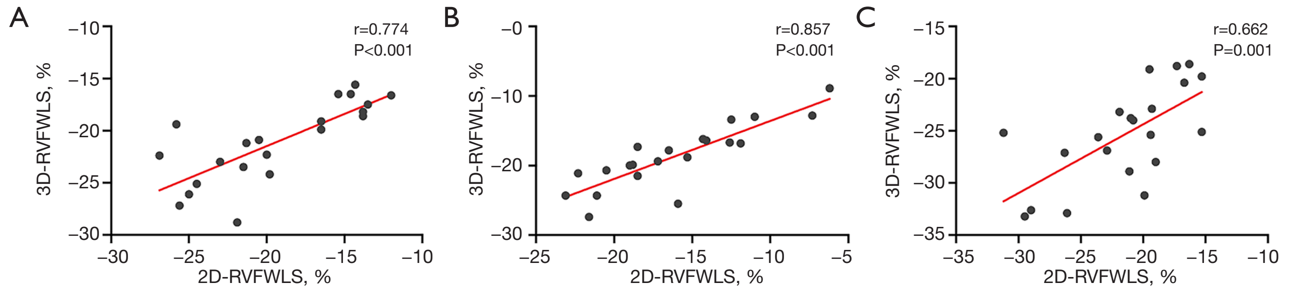

Figure 4 Correlation between 3D-RVFWLS and 2D-RVFWLS in the TPVR group. Preoperative 3D-RVFWLS was related to 2D-RVFWLS before TPVR (A), 1 week after TPVR (B), and 6 months after TPVR (C). 2D-RVFWLS, two-dimensional right ventricular free wall longitudinal strain; 3D-RVFWLS, three-dimensional right ventricular free wall longitudinal strain; TPVR, transcatheter pulmonary valve replacement.

Table 4 Correlations between 3D-RVFWLS at 6 months after TPVR and baseline echocardiographic parameters

Baseline parameter	r	P value
LVEF, %	–0.210	0.361
RVEDA, cm^2	0.271	0.234
RVESA, cm^2	0.525	0.015
RVFAC, %	–0.416	0.061
TAPSE, mm	–0.176	0.446
S', cm/s	–0.219	0.341
RVEDV, mL	0.598	0.004
RVESV, mL	0.636	0.002
RVEF, %	–0.364	0.105
2D-RVFWLS, %	0.543	0.011
3D-RVFWLS, %	0.756	<0.001

2D-RVFWLS, two-dimensional right ventricular free wall longitudinal strain; 3D-RVFWLS, three-dimensional right ventricular free wall longitudinal strain; LVEF, left ventricular ejection fraction; RVEDA, right ventricular end-diastolic area; RVEDV, right ventricular end-diastolic volume; RVEF, right ventricular ejection fraction; RVESA, right ventricular end-systolic area; RVESV, right ventricular end-systolic volume; RVFAC, right ventricular fractional area change; S', tricuspid annular systolic excursion velocity; TAPSE, tricuspid annular plane systolic excursion; TPVR, transcatheter pulmonary valve replacement.

Discussion

To the best of our knowledge, this is the first study to evaluate the changes in RV function in patients after TPVR using 3D-STE. The principal results were as follows: (I) 2D-RVFWLS and 3D-RVFWLS at 1 week after TPVR were lower than those before TPVR and improved to the baseline levels at 6 months after TPVR, but they were still lower than those of the control group. (II) Multivariate regression analysis showed that preoperative 2D-RVFWLS and 3D-RVFWLS were independent predictors of RV function and NYHA functional class at 6 months after TPVR. (III) 3D-RVFWLS was similar to 2D-RVFWLS in predicting RV function and NYHA functional class at 6 months after TPVR.

Changes in RV function after TPVR

Previous studies (27,28) have demonstrated that RV strain indices derived from 2D-STE can more accurately detect the changes in RV function as compared to conventional RV echocardiographic parameters. RV myocardial strain is independent of the geometry and angle while being less dependent on the load than conventional echocardiographic indicators. In the early stages of several cardiovascular diseases, RV free wall longitudinal strain has been shown capable of detecting subclinical RV dysfunction in the absence of changes in ejection fraction (29-31). Our findings are consistent with the results of previous studies in that 2D-RVFWLS decreased at 1 week after TPVR and gradually improved to the preoperative baseline level during the 6-month follow-up (16,32,33); however, it was lower than that in the control group. As mentioned earlier, 2D-STE is limited by the out-of-plane motion of the speckles, whereas 3D-STE can overcome this and quantify RV function more accurately and objectively in 3D space. There is no literature on the changes in RV function in 3D-STE after TPVR. Our study may be the first of its kind

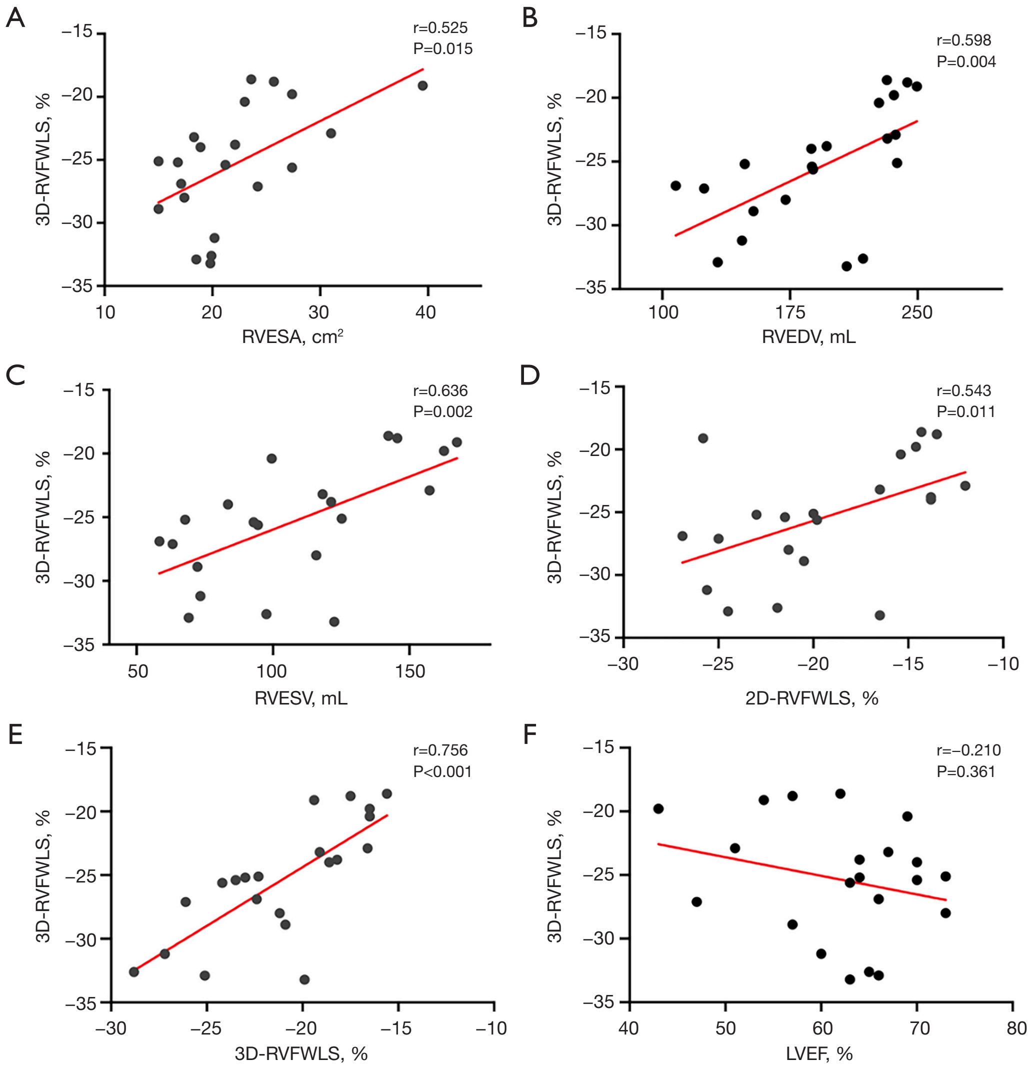

Figure 5 Correlations between 3D-RVFWLS at 6 months after TPVR and baseline parameters. 3D-RVFWLS at 6 months after TPVR was associated with preoperative RVESA (A), RVEDV (B), RVESV (C), 2D-RVFWLS (D), and 3D-RVFWLS (E) but was not correlated with preoperative LVEF (F). 2D-RVFWLS, two-dimensional right ventricular free wall longitudinal strain; 3D-RVFWLS, three-dimensional right ventricular free wall longitudinal strain; LVEF, left ventricular ejection fraction; RVEDV, right ventricular end-diastolic volume; RVESA, right ventricular end-systolic area; RVESV, right ventricular end-systolic volume; TPVR, transcatheter pulmonary valve replacement.

to evaluate RV function after TPVR using 3D-STE, and we found that 3D-RVFWLS decreased at 1 week after TPVR and recovered to the preoperative baseline level at 6 months after TPVR.

In line with the short-term follow-up results of another study (34), we found that 2D-RVFWLS and 3D-RVFWLS values decreased from preoperation to 1 week after TPVR. Strain is related to stroke volume (35), and, therefore, with the relief of PR, the reduction of RV stroke volume leads to a reduction in RV strain. In another study (34) investigating aortic valve replacement for aortic insufficiency, the observed reduction in left ventricular strain postoperatively was attributed to a mild increase in left ventricular afterload induced by the implanted prosthetic valve system. Based on this, some researchers have speculated that the transcatheter pulmonary valve system may similarly increase RV afterload, potentially contributing to the postoperative reduction in RV strain (36). However, this was not corroborated by our

Table 5 Regression analysis of 3D-RVFWLS at 6 months after TPVR

Baseline parameter	Univariate linear regression		Multivariate linear regression			
			Model I (R^2=0.424)		Model II (R^2=0.606)	
	β	P value	β	P value	β	P value
TPVR age, years	–0.147	0.525				
Age of first TOF repair, years	–0.250	0.302				
NYHA functional class	–0.283	0.214				
QRS duration, ms	0.581	<0.001				
LVEF, %	–0.257	0.262				
RVESA, cm^2	0.545	0.011				
TAPSE, mm	–0.176	0.446				
S', cm/s	–0.219	0.341				
RVEDV, mL	0.598	0.004	0.154	0.707	0.225	0.496
RVESV, mL	0.616	0.003	0.365	0.365	0.008	0.983
RVEF, %	–0.364	0.105				
2D-RVFWLS, %	0.623	0.001	0.415	0.034		
3D-RVFWLS, %	0.756	<0.001			0.618	0.008

2D-RVFWLS, two-dimensional right ventricular free wall longitudinal strain; 3D-RVFWLS, three-dimensional right ventricular free wall longitudinal strain; LVEF, left ventricular ejection fraction; NYHA, New York Heart Association; RVEDV, right ventricular end-diastolic volume; RVEF, right ventricular ejection fraction; RVESA, right ventricular end-systolic area; RVESV, right ventricular end-systolic volume; S’, tricuspid annular systolic excursion velocity; TAPSE, tricuspid annular plane systolic excursion; TOF, tetralogy of Fallot; TPVR, transcatheter pulmonary valve replacement.

findings, which indicated a decrease in RV systolic pressure after TPVR. Notably, the aforementioned study (36) on aortic valve replacement had a relatively small sample size and a specific focus on more invasive, surgical aortic valve replacement. Therefore, the impact of TPVR on RV afterload requires further investigation and validation. Another study including 10 patients with TPVR found that 2D-RVFWLS values before discharge were higher than preoperative baseline values, which was inconsistent with our findings (37). These inconsistent results may be related to the study population. The indication for TPVR in our study and that by Knirsch *et al.* was mainly due to PR (34). Among the 21 patients in our study, 17 had PR alone and 4 had PR combined with PS. However, the population in the study with relative improvement in RV strain before discharge included PS in 6 of 10 patients. A study by Lurz *et al.* using cardiac magnetic resonance imaging also reported that only patients with PS showed improvement in RVEF after TPVR, whereas RVEF did not improve immediately after TPVR or during follow-up in patients with PR (38).

Both 2D-RVFWLS and 3D-RVFWLS returned to the preoperative baseline levels at 6 months after TPVR, which was consistent with the results of a study using 2D-STE (39). The return of RV strain to baseline after TPVR may reflect RV remodeling and the gradual recovery of RV function (40). These findings are in line with those in a study on patients with aortic valve replacement for aortic regurgitation, in which postoperative strain values decreased sharply and then gradually improved (41). However, the study by Knirsch *et al.*, who used 2D-STE to evaluate the changes in RV function after surgical PVR, demonstrated that 2D-RVFWLS decreased 1 month after TPVR and gradually improved within 6 months after TPVR, but did not return to the preoperative baseline level at 6 months after surgical PVR (34). The reason for this inconsistency may be the potential irreversible myocardial damage of the RV caused by cardiopulmonary bypass. In addition, the degree of RV dilatation in the study by Knirsch *et al.* was greater than that in our study. Chronic RV volume overload leads to irreversible RV remodeling, thereby limiting the

Table 6 Univariate and multivariate regression analysis of NYHA functional class at 6 months after TPVR

Baseline parameter	Univariate linear regression		Multivariate linear regression			
			Model I (R^2=0.737)		Model II (R^2=0.771)	
	β	P value	β	P value	β	P value
TPVR age, years	0.357	0.113				
Age of first TOF repair, years	0.199	0.413				
NYHA functional class	0.250	0.274				
QRS duration, ms	0.420	0.073				
LVEF, %	–0.262	0.251				
RVESA, cm^2	0.329	0.145				
TAPSE, mm	–0.397	0.075				
S', cm/s	–0.293	0.197				
RVEDV, mL	0.605	0.004	0.559	0.051	0.128	0.643
RVESV, mL	0.713	<0.001	0.621	0.067	0.403	0.174
RVEF, %	–0.557	0.009				
2D-RVFWLS, %	0.778	<0.001	0.636	<0.001		
3D-RVFWLS, %	0.828	<0.001			0.674	<0.001

2D-RVFWLS, two-dimensional right ventricular free wall longitudinal strain; 3D-RVFWLS, three-dimensional right ventricular free wall longitudinal strain; LVEF, left ventricular ejection fraction; NYHA, New York Heart Association; RVEDV, right ventricular end-diastolic volume; RVEF, right ventricular ejection fraction; RVESA, right ventricular end-systolic area; RVESV, right ventricular end-systolic volume; S', tricuspid annular systolic excursion velocity; TAPSE, tricuspid annular plane systolic excursion; TOF, tetralogy of Fallot; TPVR, transcatheter pulmonary valve replacement.

Table 7 Intra- and interobserver variability for right ventricular free wall longitudinal strain

Variable	ICC (95% CI)	Bias (LOA)
Intraobserver		
2D-RVFWLS	0.904 (0.677, 0.975)	–0.760 (–4.368, 2.848)
3D-RVFWLS	0.935 (0.771, 0.983)	–0.500 (–2.845, 1.845)
Interobserver		
2D-RVFWLS	0.873 (0.590, 0.966)	–0.690 (–5.119, 3.739)
3D-RVFWLS	0.874 (0.591, 0.967)	–0.680 (–3.726, 2.366)

2D-RVFWLS, two-dimensional right ventricular free wall longitudinal strain; 3D-RVFWLS, three-dimensional right ventricular free wall longitudinal strain; CI, confidence interval; ICC, interclass correlation coefficient; LOA, limit of agreement.

potential for RV functional improvement after surgical PVR. Chowdhury *et al.* found that 2D-RVFWLS improved significantly at 6 months after TPVR as compared with preoperative values (16). In their study, the degree of RV dilatation in the study population was markedly lower than that in our study, and all 24 patients had moderate or severe PR with varying degrees of PS. Among them, 17 had moderate or severe PS, whereas only 4 patients in our study had PR combined with PS. In patients with PS as the primary indication for TPVR, RV afterload and stiffness are gradually reduced with the decrease in pressure and/or resistance of the pulmonary artery system after TPVR, thereby improving RV function. In addition, childhood anoxia, multiple previous cardiac surgeries, and advanced age at the time of TPVR may affect RV remodeling. Therefore, long-term follow-up is needed to observe whether the RV function can gradually improve from preoperative levels in patients after TPVR.

Predictive value of 3D-RVFWLS

In recent years, a growing number of studies have demonstrated that 2D-RVFWLS is capable of quantifying RV performance and providing prognostic information.

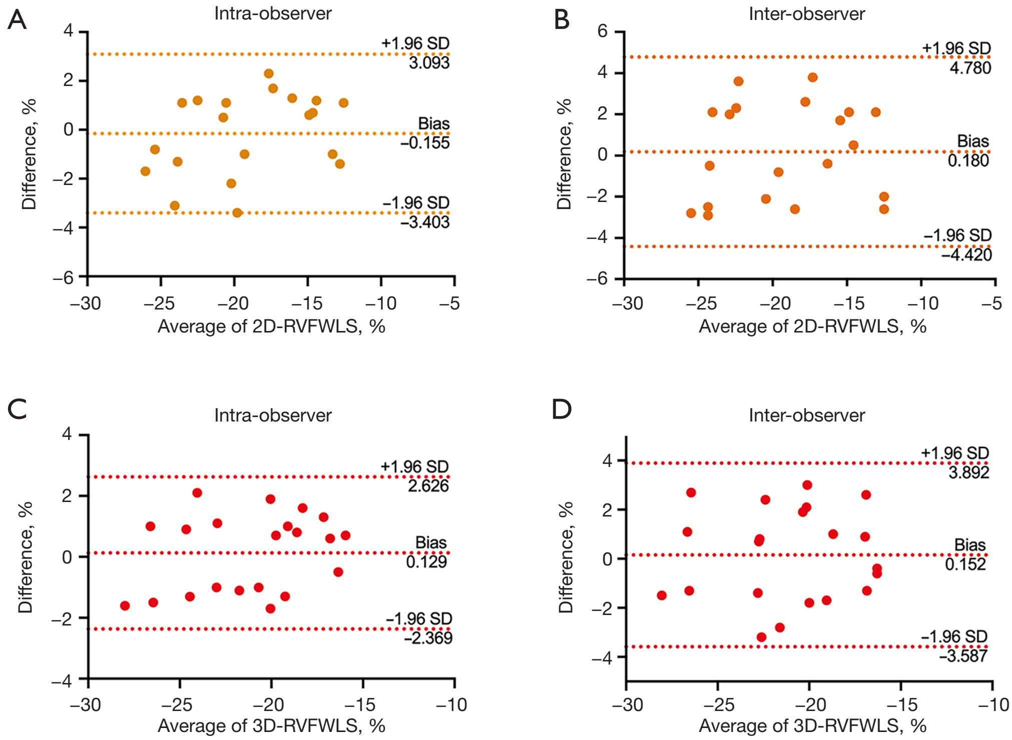

Figure 6 Bland-Altman analysis of 2D-RVFWLS and 3D-RVFWLS. Bland-Altman analysis demonstrated the high intraobserver (A) and interobserver (B) agreement of 2D-RVFWLS. Bland-Altman analysis demonstrated the high intraobserver (C) and interobserver (D) agreement of 3D-RVFWLS. 2D-RVFWLS, two-dimensional right ventricular free wall longitudinal strain; 3D-RVFWLS, three-dimensional right ventricular free wall longitudinal strain; SD, standard deviation.

Sabate Rotes *et al.* carried out a study using 2D-STE in patients with surgical PVR and found that better preoperative 2D-RVFWLS was an independent predictor of higher 2D-RVFWLS at 1 year after surgery (32). Univariate regression analysis showed that better 2D-RVFWLS before operation was a predictor of NYHA functional class ≥II at a mean follow-up of 8 months after operation. In the study by Chowdhury *et al.* the ventilatory efficiency derived from exercise testing, the slope of minute ventilation ($\dot{V}_E$)/carbon dioxide production ($\dot{V}_{CO_2}$), was a predictive indicator of mortality (42). The patients with lower 2D-RVFWLS values before TPVR showed the most significant improvement in $\dot{V}_E/\dot{V}_{CO_2}$ after TPVR, and 2D-RVFWLS before TPVR was closely correlated with the percentage change in $\dot{V}_E/\dot{V}_{CO_2}$ after TPVR. Hasan *et al.* applied 2D-STE to evaluate ventricular function in 20 patients with an obstructed RV outflow tract conduit, and they found that higher 2D-RVFWLS before intervention was associated with higher 2D-RVFWLS after TPVR, suggesting that the better RV function before TPVR may be related to the benefit of removing obstructions to the RV function after TPVR (43). However, there are several inherent limitations of 2D-STE, and 3D-STE can theoretically overcome these shortcomings. Thus, a direct comparison between 2D-RVFWLS and 3D-RVFWLS for predicting RV function and NYHA functional class after TPVR holds considerable clinical significance.

Several studies have investigated the prognostic significance of RV strain on 3D-STE in patients with pulmonary hypertension (18,44). However, few have directly compared the utility of 2D-STE and 3D-STE in RV function evaluation. One study indicated that 2D-RVFWLS and 3D-RVFWLS are independently related to poor clinical outcomes in patients with heart failure and preserved ejection fraction (45). The multivariate Cox hazard model in this study demonstrated that there is similar prognostic value between 3D-RVFWLS and 2D-RVFWLS (45). Similarly, our findings revealed that both 2D-RVFWLS and 3D-RVFWLS were independently associated with RV function and NYHA functional class at the 6-month follow-up after TPVR. Moreover, our multivariate linear regression analysis further indicated that 3D-RVFWLS had comparable predictive power to 2D-RVFWLS. To our knowledge, this is the first study to evaluate the predictive significance of 3D-RVFWLS in patients with TPVR and to directly compare its value with that of the 2D-RVFWLS. Overall, our study reinforces and extends previous observations by demonstrating the clinical application of RV strain analysis in the risk stratification of patients scheduled for TPVR. Importantly, we not only confirmed the prognostic significance of 2D-RVFWLS and 3D-RVFWLS in patients with TPVR but also demonstrated that 3D-STE and 2D-STE parameters have a similar ability to predict RV function and NYHA functional class after TPVR.

Clinical implications

Preoperative 2D-RVFWLS and 3D-RVFWLS are independent predictors of RV function and NYHA functional class at 6 months after TPVR. For patients scheduled to undergo TPVR, using the normal reference range of RVFWLS for the accurate assessment of RV function is helpful for clinicians in identifying high-risk patients with poor postoperative prognosis. However, there is a lack of comprehensive normative data for 3D-RVFWLS, with most existing reference values derived from small samples comprising healthy individuals. Additionally, variations in measurement algorithms across different platforms can lead to inconsistencies in reference ranges. Due to these limitations and the scarcity of robust data, 3D-RVFWLS reference values are not yet suitable for routine clinical application. More importantly, our study showed that 3D-RVFWLS was similar to 2D-RVFWLS in predicting RV function and NYHA functional class at 6 months after TPVR. This is critical because the widespread use of 3D-RVFWLS is restrained by a lack of training and/or compatible equipment. In contrast, 2D-RVFWLS is widely applied for quantify RV function in clinical practice in most echocardiography laboratories. Therefore, for patients with preoperative RV strain below the normal reference range, defined as a 2D-RVFWLS value is less than −20% (46), the timing of TPVR should be appropriately delayed. Medical therapy should be initiated first to alleviate symptoms and improve RV function, and surgical intervention should be deferred until RV function has normalized. This can avoid postoperative RV function deterioration and the occurrence of adverse cardiovascular events involving malignant arrhythmias, heart failure, and even sudden cardiac death, thereby improving the prognosis of patients and prolonging their expected lifespan.

Limitations

Several limitations of this present study merit discussion. First, as we employed a single-center study with a small sample size, our findings require further validation in multicenter studies with larger sample sizes. Second, the follow-up period was relatively short, and the long-term impact of TPVR on RV function should be further investigated. Third, the effect of TPVR on RV function may be different in patients with PR alone and PR combined with PS. Fourth, age at TOF repair and age at TPVR may influence the postoperative RV function. However, the sample size in this study was too small to allow for a meaningful subgroup analysis. Finally, 3D-STE has low temporal resolution and is highly dependent on image quality; therefore, patients with suboptimal image quality were excluded from our study.

Future directions

TPVR is of considerable significance for patients at high risk or with contraindications to surgical PVR. Accurate assessment of RV function is critical in the treatment of patients before TPVR. However, the majority of studies on this subject have focused on the changes in 2D-RVFWLS after TPVR, and reports on the application of 3D-RVFWLS to evaluate the changes in RV function in patients before and after TPVR are lacking. Although our study has addressed this deficiency to an extent, given the aforementioned limitations of the study, there is still considerable potential for future research on patients with TPVR. First, we need to conduct studies involving multiple centers with larger sample sizes and longer follow-up periods to confirm the impact of TPVR on RV function and prognosis information. This will further clarify the relative value of 2D-RVFWLS and 3D-RVFWLS in predicting major adverse cardiovascular events. Second, the indications for TPVR include three types: PR, PS, and PR combined with PS. Due to the fact that the changes in RV pressure load and volume load before and after TPVR are not completely consistent for these three types of patients, the effect of TPVR on the RV function of these patients may also vary to some extent. Therefore, future studies should attempt to separately examine the effects of

TPVR on RV function in patients with PR, PS, and PR combined with PS, respectively. Third, myocardial work is another complex indicator for evaluating ventricular function, and RV myocardial work also takes into account the influence of RV afterload and consequent measurement correction (47-50). Therefore, the effects of RV strain and RV myocardial work should be jointly investigated in future work. In conclusion, future research directions should involve a more comprehensive inclusion of factors that affect the RV function in patients treated with TPVR and greater objectivity in identifying the predictive factors of RV function and adverse prognosis. In this way, clinicians can be better informed in making decisions related to individualized treatment.

Conclusions

One week after TPVR, 2D-RVFWLS and 3D-RVFWLS are decreased, and return to the baseline levels at 6 months. Preoperative 3D-RVFWLS is an independent predictor of RV function and NYHA functional class at 6 months after TPVR, providing similar value to that of 2D-RVFWLS in determining the optimal timing of TPVR.

Acknowledgments

We would like to thank our colleagues for supporting our research. The preliminary findings of this research have been shared as a poster presentation at the American Society of Echocardiography 35th Annual Scientific Sessions held in Portland, Oregon, America on June 14-16, 2024 [https://onlinejase.com/article/S0894-7317(24)00188-3/fulltext].

Footnote

Reporting Checklist: The authors have completed the STROBE reporting checklist. Available at https://qims.amegroups.com/article/view/10.21037/qims-2025-863/rc

Data Sharing Statement: Available at https://qims.amegroups.com/article/view/10.21037/qims-2025-863/dss

Funding: This study was funded by the National Natural Science Foundation of China (Nos. 82371991, 82230066, 82201408, 82302225, and 82402002).

Conflicts of Interest: All authors have completed the ICMJE uniform disclosure form (available at https://qims.amegroups.com/article/view/10.21037/qims-2025-863/coif). The authors have no conflicts of interest to declare.

Ethical Statement: The authors are accountable for all aspects of the work in ensuring that questions related to the accuracy or integrity of any part of the work are appropriately investigated and resolved. The study was conducted in accordance with the Declaration of Helsinki and its subsequent amendments. This study was approved by the Ethics Committee of Wuhan Union Hospital, Tongji Medical College, Huazhong University of Science and Technology (No. UHCT-IEC-SOP-016-03-03) and informed consent was taken from all individual participants.

References

1. Meca Aguirrezabalaga JA, Silva Guisasola J, Díaz Méndez R, Escalera Veizaga AE, Hernández-Vaquero Panizo D. Pulmonary regurgitation after repaired tetralogy of Fallot: surgical versus percutaneous treatment. Ann Transl Med 2020;8:967.
2. Mikhail A, Labbio GD, Darwish A, Kadem L. How pulmonary valve regurgitation after tetralogy of fallot repair changes the flow dynamics in the right ventricle: An in vitro study. Med Eng Phys 2020;83:48-55.
3. Mauger CA, Govil S, Chabiniok R, Gilbert K, Hegde S, Hussain T, McCulloch AD, Occleshaw CJ, Omens J, Perry JC, Pushparajah K, Suinesiaputra A, Zhong L, Young AA. Right-left ventricular shape variations in tetralogy of Fallot: associations with pulmonary regurgitation. J Cardiovasc Magn Reson 2021;23:105.
4. Park WY, Kim GB, Lee SY, Song MK, Kwon HW, An HS, Bae EJ, Cho S, Kwak JG, Kim WH. Long-Term Outcome and Risk Factor Analysis of Surgical Pulmonary Valve Replacement in Congenital Heart Disease. Congenital Heart Disease 2022;17:335-50.
5. Ho JP, Ng CW, Wong WH, Cheung YF. Cardiothoracic Ratio for Assessment of Ventricular Volumes and Function

in Patients with Repaired Tetralogy of Fallot. Congenital Heart Disease 2025;20:201-11.
6. Bedzra E, Contorno E, Javed H, Qasim A, Louis JS, Rajab TK. Tetralogy of Fallot: Anatomy, Physiology, and Outcomes. Congenital Heart Disease 2024;19:541-62.
7. Alkashkari W, Albugami S, Abbadi M, Niyazi A, Alsubei A, Hijazi ZM. Transcatheter pulmonary valve replacement in pediatric patients. Expert Rev Med Devices 2020;17:541-54.
8. Jalal Z, Valdeolmillos E, Malekzadeh-Milani S, Eicken A, Georgiev S, Hofbeck M, Sieverding L, Gewillig M, Ovaert C, Bouvaist H, Pillois X, Thambo JB, Boudjemline Y. Mid-Term Outcomes Following Percutaneous Pulmonary Valve Implantation Using the "Folded Melody Valve" Technique. Circ Cardiovasc Interv 2021;14:e009707.
9. Zhang JN, Wan JY, Li YH, Han Y, Pan JH, Fang F, Jiang SL, Pan XB, Zhang GJ. Outcomes of Self-Expanding Transcatheter Pulmonary Valves: Extended Follow-Up of a Prospective Trial. Congenital Heart Disease 2023;18:219-34.
10. Castaldi B, Prati F, Pozza A, Cattapan I, Fumanelli J, Sirico D, Salvo GD. Transcatheter Pulmonary Valve Implantation: A State of the Art Review. Congenital Heart Disease 2024;19:513-33.
11. Baumgartner H, De Backer J, Babu-Narayan SV, Budts W, Chessa M, Diller GP, Lung B, Kluin J, Lang IM, Meijboom F, Moons P, Mulder BJM, Oechslin E, Roos-Hesselink JW, Schwerzmann M, Sondergaard L, Zeppenfeld K; ESC Scientific Document Group. 2020 ESC Guidelines for the management of adult congenital heart disease. Eur Heart J 2021;42:563-645.
12. Tian F, Zhang L, Xie Y, Zhang Y, Zhu S, Wu C, Sun W, Li M, Gao Y, Wang B, Wang J, Yang Y, Lv Q, Dong N, Li Y, Xie M. 3-Dimensional Versus 2-Dimensional STE for Right Ventricular Myocardial Fibrosis in Patients With End-Stage Heart Failure. JACC Cardiovasc Imaging 2021;14:1309-20.
13. Zhang XL, Peng Y. Echocardiographic Assessment Progress of Pulmonary Regurgitation after Surgical Repair of Tetralogy of Fallot. Adv Cardiovasc Dis 2018;39:316-9.
14. Vijiiac A, Onciul S, Guzu C, Scarlatescu A, Petre I, Zamfir D, Onut R, Deaconu S, Dorobantu M. Forgotten No More-The Role of Right Ventricular Dysfunction in Heart Failure with Reduced Ejection Fraction: An Echocardiographic Perspective. Diagnostics (Basel) 2021;11:548.
15. Landzaat JWD, van Heerebeek L, Jonkman NH, van der Bijl EM, Riezebos RK. The quest for determination of standard reference values of right ventricular longitudinal systolic strain: a systematic review and meta-analysis. J Echocardiogr 2023;21:1-15.
16. Chowdhury SM, Hijazi ZM, Rhodes JF, Kar S, Makkar R, Mullen M, Cao QL, Mandinov L, Buckley J, Pietris NP, Shirali GS. Changes in speckle tracking echocardiography measures of ventricular function after percutaneous implantation of the Edwards SAPIEN transcatheter heart valve in the pulmonary position. Echocardiography 2015;32:461-9.
17. Sciaccaluga C, D'Ascenzi F, Mandoli GE, Rizzo L, Sisti N, Carrucola C, Cameli P, Bigio E, Mondillo S, Cameli M. Traditional and Novel Imaging of Right Ventricular Function in Patients with Heart Failure and Reduced Ejection Fraction. Curr Heart Fail Rep 2020;17:28-33.
18. Li Y, Wang T, Haines P, Li M, Wu W, Liu M, Chen Y, Jin Q, Xie Y, Wang J, Yang Y, Zhang L, Lv Q, Xie M. Prognostic Value of Right Ventricular Two-Dimensional and Three-Dimensional Speckle-Tracking Strain in Pulmonary Arterial Hypertension: Superiority of Longitudinal Strain over Circumferential and Radial Strain. J Am Soc Echocardiogr 2020;33:985-994.e1.
19. Gummadi S, Eisenbrey J, Li J, Li Z, Forsberg F, Lyshchik A, Liu JB. Advances in Modern Clinical Ultrasound. Advanced Ultrasound in Diagnosis and Therapy 2018;2:51-63.
20. Zahn EM, Hellenbrand WE, Lock JE, McElhinney DB. Implantation of the melody transcatheter pulmonary valve in patients with a dysfunctional right ventricular outflow tract conduit early results from the u.s. Clinical trial. J Am Coll Cardiol 2009;54:1722-9.
21. Feltes TF, Bacha E, Beekman RH 3rd, Cheatham JP, Feinstein JA, Gomes AS, Hijazi ZM, Ing FF, de Moor M, Morrow WR, Mullins CE, Taubert KA, Zahn EM; American Heart Association Congenital Cardiac Defects Committee of the Council on Cardiovascular Disease in the Young; Council on Clinical Cardiology; Council on Cardiovascular Radiology and Intervention; American Heart Association. Indications for cardiac catheterization and intervention in pediatric cardiac disease: a scientific statement from the American Heart Association. Circulation 2011;123:2607-52.
22. Mitchell C, Rahko PS, Blauwet LA, Canaday B, Finstuen JA, Foster MC, Horton K, Ogunyankin KO, Palma RA, Velazquez EJ. Guidelines for Performing a Comprehensive Transthoracic Echocardiographic Examination in Adults: Recommendations from the American Society of Echocardiography. J Am Soc Echocardiogr 2019;32:1-64.
23. Lang RM, Badano LP, Mor-Avi V, Afilalo J, Armstrong A, Ernande L, Flachskampf FA, Foster E, Goldstein SA,

Kuznetsova T, Lancellotti P, Muraru D, Picard MH, Rietzschel ER, Rudski L, Spencer KT, Tsang W, Voigt JU. Recommendations for cardiac chamber quantification by echocardiography in adults: an update from the American Society of Echocardiography and the European Association of Cardiovascular Imaging. J Am Soc Echocardiogr 2015;28:1-39.e14.
24. Humbert M, Kovacs G, Hoeper MM, Badagliacca R, Berger RMF, Brida M, et al. 2022 ESC/ERS Guidelines for the diagnosis and treatment of pulmonary hypertension. Eur Heart J 2022;43:3618-731. Erratum in: Eur Heart J 2023;44:1312.
25. Puchalski MD, Askovich B, Sower CT, Williams RV, Minich LL, Tani LY. Pulmonary regurgitation: determining severity by echocardiography and magnetic resonance imaging. Congenit Heart Dis 2008;3:168-75.
26. Mercer-Rosa L, Yang W, Kutty S, Rychik J, Fogel M, Goldmuntz E. Quantifying pulmonary regurgitation and right ventricular function in surgically repaired tetralogy of Fallot: a comparative analysis of echocardiography and magnetic resonance imaging. Circ Cardiovasc Imaging 2012;5:637-43.
27. Carluccio E, Biagioli P, Alunni G, Murrone A, Zuchi C, Coiro S, Riccini C, Mengoni A, D'Antonio A, Ambrosio G. Prognostic Value of Right Ventricular Dysfunction in Heart Failure With Reduced Ejection Fraction: Superiority of Longitudinal Strain Over Tricuspid Annular Plane Systolic Excursion. Circ Cardiovasc Imaging 2018;11:e006894.
28. Gorter TM, van Veldhuisen DJ, Bauersachs J, Borlaug BA, Celutkiene J, Coats AJS, et al. Right heart dysfunction and failure in heart failure with preserved ejection fraction: mechanisms and management. Position statement on behalf of the Heart Failure Association of the European Society of Cardiology. Eur J Heart Fail 2018;20:16-37.
29. Galderisi M, de Simone G, Innelli P, Turco A, Turco S, Capaldo B, Riccardi G, de Divitiis O. Impaired inotropic response in type 2 diabetes mellitus: a strain rate imaging study. Am J Hypertens 2007;20:548-55.
30. Morris DA, Krisper M, Nakatani S, Köhncke C, Otsuji Y, Belyavskiy E, Radha Krishnan AK, Kropf M, Osmanoglou E, Boldt LH, Blaschke F, Edelmann F, Haverkamp W, Tschöpe C, Pieske-Kraigher E, Pieske B, Takeuchi M. Normal range and usefulness of right ventricular systolic strain to detect subtle right ventricular systolic abnormalities in patients with heart failure: a multicentre study. Eur Heart J Cardiovasc Imaging 2017;18:212-23.
31. Li Y, Xie M, Wang X, Lv Q, Lu X, Yang Y, Ma H, Fang L, Zhang J, Li W. Evaluation of right ventricular global longitudinal function in patients with tetralogy of fallot by two-dimensional ultrasound speckle tracking imaging. J Huazhong Univ Sci Technolog Med Sci 2010;30:126-31.
32. Sabate Rotes A, Bonnichsen CR, Reece CL, Connolly HM, Burkhart HM, Dearani JA, Eidem BW. Long-term follow-up in repaired tetralogy of fallot: can deformation imaging help identify optimal timing of pulmonary valve replacement? J Am Soc Echocardiogr 2014;27:1305-10.
33. Pagourelias ED, Daraban AM, Mada RO, Duchenne J, Mirea O, Cools B, Heying R, Boshoff D, Bogaert J, Budts W, Gewillig M, Voigt JU. Right ventricular remodelling after transcatheter pulmonary valve implantation. Catheter Cardiovasc Interv 2017;90:407-17.
34. Knirsch W, Dodge-Khatami A, Kadner A, Kretschmar O, Steiner J, Böttler P, Kececioglu D, Harpes P, Valsangiacomo Buechel ER. Assessment of myocardial function in pediatric patients with operated tetralogy of Fallot: preliminary results with 2D strain echocardiography. Pediatr Cardiol 2008;29:718-25.
35. Jamal F, Bergerot C, Argaud L, Loufouat J, Ovize M. Longitudinal strain quantitates regional right ventricular contractile function. Am J Physiol Heart Circ Physiol 2003;285:H2842-7.
36. Pomerantz BJ, Krock MD, Wollmuth JR, Cupps BP, Kouchoukos NT, Davila-Roman VG, Pasque MK. Aortic valve replacement for aortic insufficiency: valve type as a determinant of systolic strain recovery. J Card Surg 2005;20:524-9.
37. Moiduddin N, Asoh K, Slorach C, Benson LN, Friedberg MK. Effect of transcatheter pulmonary valve implantation on short-term right ventricular function as determined by two-dimensional speckle tracking strain and strain rate imaging. Am J Cardiol 2009;104:862-7.
38. Lurz P, Nordmeyer J, Giardini A, Khambadkone S, Muthurangu V, Schievano S, Thambo JB, Walker F, Cullen S, Derrick G, Taylor AM, Bonhoeffer P. Early versus late functional outcome after successful percutaneous pulmonary valve implantation: are the acute effects of altered right ventricular loading all we can expect? J Am Coll Cardiol 2011;57:724-31.
39. Moiduddin N, Texter KM, Cheatham JP, Chisolm JL, Kovalchin JP, Nicholson L, Belfrage KM, Janevski I, Cua CL. Strain echocardiographic assessment of ventricular function after percutaneous pulmonary valve implantation. Congenit Heart Dis 2012;7:361-71.
40. Wranne B, Pinto FJ, Hammarström E, St Goar FG, Puryear J, Popp RL. Abnormal right heart filling after

cardiac surgery: time course and mechanisms. Br Heart J 1991;66:435-42.
41. Becker M, Kramann R, Dohmen G, Lückhoff A, Autschbach R, Kelm M, Hoffmann R. Impact of left ventricular loading conditions on myocardial deformation parameters: analysis of early and late changes of myocardial deformation parameters after aortic valve replacement. J Am Soc Echocardiogr 2007;20:681-9.
42. Chowdhury SM, Hijazi ZM, Fahey JT, Rhodes JF, Kar S, Makkar R, Mullen M, Cao QL, Shirali GS. Speckle-Tracking Echocardiographic Measures of Right Ventricular Function Correlate With Improvement in Exercise Function After Percutaneous Pulmonary Valve Implantation. J Am Soc Echocardiogr 2015;28:1036-44.
43. Hasan BS, Lunze FI, Chen MH, Brown DW, Boudreau MJ, Rhodes J, McElhinney DB. Effects of transcatheter pulmonary valve replacement on the hemodynamic and ventricular response to exercise in patients with obstructed right ventricle-to-pulmonary artery conduits. JACC Cardiovasc Interv 2014;7:530-42.
44. Vitarelli A, Mangieri E, Terzano C, Gaudio C, Salsano F, Rosato E, Capotosto L, D'Orazio S, Azzano A, Truscelli G, Cocco N, Ashurov R. Three-dimensional echocardiography and 2D-3D speckle-tracking imaging in chronic pulmonary hypertension: diagnostic accuracy in detecting hemodynamic signs of right ventricular (RV) failure. J Am Heart Assoc 2015;4:e001584.
45. Meng Y, Zhu S, Xie Y, Zhang Y, Qian M, Gao L, Li M, Lin Y, Wu W, Wang J, Yang Y, Lv Q, Zhang L, Li Y, Xie M. Prognostic Value of Right Ventricular 3D Speckle-Tracking Strain and Ejection Fraction in Patients With HFpEF. Front Cardiovasc Med 2021;8:694365.
46. Mukherjee M, Rudski LG, Addetia K, Afilalo J, D'Alto M, Freed BH, Friend LB, Gargani L, Grapsa J, Hassoun PM, Hua L, Kim J, Mercurio V, Saggar R, Vonk-Noordegraaf A. Guidelines for the Echocardiographic Assessment of the Right Heart in Adults and Special Considerations in Pulmonary Hypertension: Recommendations from the American Society of Echocardiography. J Am Soc Echocardiogr 2025;38:141-86.
47. Butcher SC, Fortuni F, Montero-Cabezas JM, Abou R, El Mahdiui M, van der Bijl P, van der Velde ET, Ajmone Marsan N, Bax JJ, Delgado V. Right ventricular myocardial work: proof-of-concept for non-invasive assessment of right ventricular function. Eur Heart J Cardiovasc Imaging 2021;22:142-52.
48. Landra F, Sciaccaluga C, Pastore MC, Gallone G, Barilli M, Fusi C, Focardi M, Cavigli L, D'Ascenzi F, Natali BM, Bernazzali S, Maccherini M, Valente S, Cameli M, Mandoli GE. Right ventricular myocardial work for the prediction of early right heart failure and long-term mortality after left ventricular assist device implant. Eur Heart J Cardiovasc Imaging 2023;25:105-15.
49. Russell K, Eriksen M, Aaberge L, Wilhelmsen N, Skulstad H, Remme EW, Haugaa KH, Opdahl A, Fjeld JG, Gjesdal O, Edvardsen T, Smiseth OA. A novel clinical method for quantification of regional left ventricular pressure-strain loop area: a non-invasive index of myocardial work. Eur Heart J 2012;33:724-33.
50. Landra F, Mandoli GE, Chiantini B, Barilli M, Merello G, De Carli G, Sciaccaluga C, Lisi M, Flamigni F, D'Ascenzi F, Focardi M, Fineschi M, Iadanza A, Bernazzali S, Maccherini M, Valente S, Cameli M. Correlation of left ventricular myocardial work indices with invasive measurement of stroke work in patients with advanced heart failure. Front Cardiovasc Med 2022;9:946540.

Cite this article as: Ji M, Wu W, Xie M, Zhang L, Lin Y, Gao L, He Q, Dong N, Li Y. Changes in right ventricular function on three-dimensional speckle tracking echocardiography after transcatheter pulmonary valve replacement. Quant Imaging Med Surg 2025;15(11):10886-10904. doi: 10.21037/qims-2025-863